Global Journal of Engineering and Technology Advances
eISSN: 2582-5003
Cross Ref DOI: 10.30574/gjeta
Journal homepage: https://gjeta.com/
GJETA

(Research Article)

Check for updates

Experimental validation of open-motor derived ballistic models for propellant grain burn dynamics

Gbadebo Omoniyi Adeniyi [1,*], Samuel Okemute Egwenu [1], David Oluwasegun Kolade [2], Olubukola Esther Olowu [1] and Adeoye Robert Adedeji [1]

[1] Rocket Propellant Development Systems, Bola Ahmed Tinubu Centre for Space Transport and Propulsion, LASU Epe Campus, Lagos, Nigeria.
[2] Department of Aerospace Engineering, Faculty of Engineering, Lagos State University, Epe, Lagos, Nigeria.

Global Journal of Engineering and Technology Advances, 2026, 28(01), 001-012

Publication history: Received on 18 May 2026; revised on 29 June 2026; accepted on 01 July 2026

Article DOI: https://doi.org/10.30574/gjeta.2026.28.1.0167

Abstract

This study evaluated the ballistic performance of four propellant grain geometries (star, Bate, finocyl, and rod-and-tube) using Open-Motor software, with results validated via static testing. Grain geometry dictates internal ballistics by governing the burning surface area, directly controlling chamber pressure, mass flow rate, and thrust. Star grain propellant geometry yields an intense progressive-short neutral-regressive profile with the highest peak pressure and thrust, but the shortest burn duration. Finocyl propellant grain geometry provides a balanced, mildly progressive-to-regressive-neutral profile. Bate and Rod and Tube propellant grain geometries, deliver neutral burn profiles by balancing internal and external surfaces. The Bate grain ensures high burn efficiency and steady pressure, while the rod-and-tube configuration maximizes burn longevity at a reduced thrust magnitude.

Ultimately, these findings demonstrate how geometric design can precisely tailor a motor's ballistic profile-optimizing either for the rapid, high-magnitude thrust needed by tactical interceptors, or the sustained, uniform thrust required for booster stages. Open-Motor is a suitable tool for evaluating diverse propellant grain geometries characteristic on motor ballistics.

Keywords: Grain Geometry Design; Ballistic Test Parameters; Thrust-Time Profile; Progressive; Regressive; Neutral Burning Pattern; Burning Surface Area; Bates, Finocyl; Star and Rod – and – Tube Grains

1. Introduction

Solid rocket motors (SRMs) play a crucial role in modern aerospace and Defence systems because of their simplicity, reliability, and high thrust-to-weight ratio (Korompili et al., 2024). A solid-propellant rocket motor consists of a casing, usually steel, filled with a solid propellant charge, called the grain, which contains all the chemical constituents (fuel plus oxidizer) for complete burning, the nozzle, internal insulation and the ignitor (Mohamed et al., 2018). Solid propellant grain are the thrust generation devices and core load-bearing components of solid rocket motor (SRM) and are also known as SRM grain. They are constantly exposed to extreme service environments such as high temperatures, high pressures, and dynamic shocks, and have a relatively high failure rate in the field use of SRM (Tang et al. 2025). The performance of an SRM is primarily determined by the combustion of a solid propellant grain enclosed within a motor casing, where chemical energy is converted into high-pressure gases that are expelled through a nozzle to generate thrust. The internal ballistic performance of a solid rocket motor depends on several interrelated parameters, including chamber pressure, propellant burn rate, mass flow rate, and thrust-time characteristics These parameters are

* Corresponding author: Gbadebo Omoniyi Adeniyi.

strongly influenced by the geometry of the propellant grain, which governs how the burning surface evolves during combustion (Sutton and Biblarz, 2017).

As the propellant burns and regresses inward, the available surface area changes with time, directly affecting the pressure history inside the combustion chamber. This relationship determines whether the motor exhibits regressive, neutral, or progressive thrust behaviour, each of which is suited to different mission requirements (Sutton and Biblarz, 2017). Consequently, grain geometry is a fundamental design variable in achieving desired performance outcomes (Gupta et al., 2020). Different propellant grain geometries maintain near-constant chamber pressure or generate specific thrust-time patterns required for stable flight and payload delivery (Sutton and Biblarz, 2017). The design and analysis of propellant grain configurations is a crucial step in the design of solid propellant rocket motors. This is because the performance prediction relies on accurate calculations of grain geometrical properties (Nehal and Venkatachalam, 2024). The design of such grains requires a careful balance between performance optimization, manufacturability, and structural integrity (Nehal and Venkatachalam, 2024). Therefore, understanding the influence of propellant grain geometry is essential for the safe and efficient design of solid rocket motors. Grain shape not only affects ballistic performance but also impacts thermal loading, mechanical stresses, and overall motor reliability. A systematic investigation of different grain geometries helps engineers predict performance trends and select appropriate configurations for specific applications (Gupta et al., 2020). Such knowledge is particularly valuable during the early stages of design, where informed decisions can reduce development costs and improve mission success.

2. Material and methods

2.1. Description of the Experiment

The theoretical simulation of the various internal ballistic of different propellant grains were carried out using Open-Motor. The propellant grain geometries of interest were Bate, Star, Finocyl, and Rod-and-Tube grains (Figure 1). 0.85 kg KNSB propellant was produced for each type of the selected propellant grain geometry (Bate, Star, Finocyl, and Rod-and-Tube grains) (Figure 2). Each of the samples were loaded in the rocket motor (Figure 3) for static ballistic test using ballistic evaluator. The experiments were carried out under identical propellant and nozzle conditions to carry out experimental static firing test to validate the predicted parameters by the open-motor. The ballistic parameters of interests were: chamber pressure, thrust-time profile, burn rate, total impulse and specific impulse.

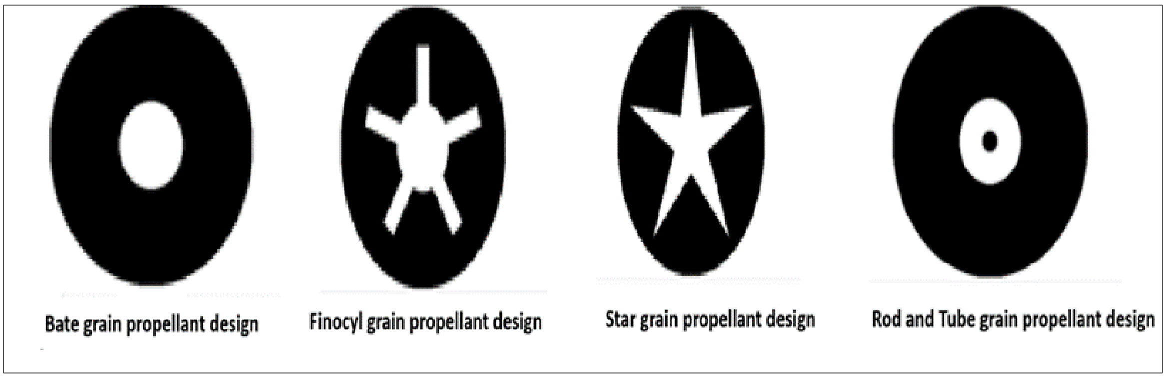

Figure 1 The selected propellant grain geometries

Figure 2 Four different propellant grain geometries manufactured for tests

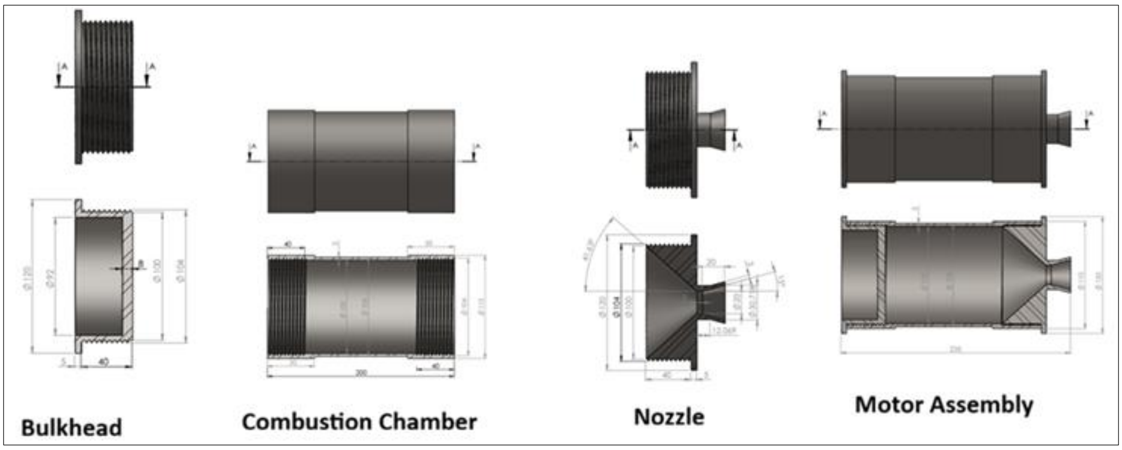

Figure 3 The rocket motor used for the experiment

2.2. Grain Geometries Design Specifications

The designed grain geometry samples fixtures selected for the empirical measurements are as shown in Table 1-4. The grain geometries were designed or modelled to determine the instantaneous burning surface area as a function of regression distance.

Table 1 Bates Grain Design Fixtures

S/N	Grain Parameters	Units	Value
1	Propellant mass	kg	0.85
2	Propellant Outer diameter	m	0.08
3	Propellant core diameter	m	0.025
4	Propellant length	m	0.107

Table 2 Finocyl Grain Design Fixtures

S/N	Grain Parameters	Units	Value
1	Propellant mass	kg	0.85
2	Propellant Outer diameter	m	0.08
3	Propellant core diameter	m	0.025
4	Propellant length	m	0.12
5	Number of fins	-	5
6	Fin width	m	0.006
7	Fin length	m	0.016

Table 3 Star Grain Design Fixtures

S/N	Grain Parameters	Units	Value
1	Propellant mass	kg	0.85
2	Propellant Outer diameter	m	0.08
3	Propellant length	m	0.12
4	Number of star points	-	5
5	Point length	m	0.035
6	Point base width	m	0.015

Table 4 Rod and Tube Grain Design Fixtures

S/N	Grain Parameters	Units	Value
1	Propellant mass	kg	0.85
2	Propellant Outer diameter	m	0.08
3	Propellant length	m	0.107
4	Propellant core diameter	m	0.025
5	Rod diameter	m	0.006

2.3. The Experimental Set-up

The ballistic evaluation method set-up consisted of a combustion chamber with instrumented casing, nozzle assembly, load cell (for thrust measurement) and data acquisition system (Ghelichkhani et al. 2025). The Experiments were carried out at the premises of the Bola Ahmed Tinubu Centre for Space Transport and Propulsion, Epe, Lagos State, Nigeria. During the combustion process, the thrust generated was sensed as an electrical signal by the load cell and recorded by the data acquisition module which served as an intermediary between the load cell and the laptop where the signals were collected as data, filtered and processed to obtain reliable values. The Thrust and burn time were measured using a data acquisition facility which can measure up to 2000 N thrust with 0.037% accuracy.

The delivered average thrust and maximum thrust, propellant burn time (the actual and average propellant burn-out time) and the chamber pressure (maximum chamber pressure and aaverage chamber pressure) were obtained from the experiment. The propellant specific impulse, total impulse and burn rate were derived from the measured empirical values.

3. Results and discussion

The Open-Motor simulated ballistic and delivered empirical values are presented with their corresponding thrust profiles in Tables 5 – 10 and Figures 4 - 11. The simulated prediction of the average thrust, maximum thrust, specific impulse, the propellant burn time, the total impulse, the average chamber pressure and maximum chamber pressure for Bate grain propellant design are: 261.54N, 303.38N,99.76s, 3.15s, 830.89Ns, 0.75MPa, 0.87MPa (Table 5) correspondingly. The delivered average thrusts, specific impulse, thrust, maximum thrust, the propellant burn time, the total impulse, the average chamber pressure and maximum chamber pressure were: 272.90N, 324.35N,89.67s, 2.74s, 747.75Ns, 0.72MPa, 0.85MPa.Table 6 also presented correspondingly both the theoretical prediction and the measured ballistic parameters(thrust, maximum thrust, specific impulse, the propellant burn time, the total impulse, the average chamber pressure and maximum chamber pressure) for Finocyl grain geometry follows: 396.28N (307.41N), 553.30N (573.63N), 100.36s(89.21s), 2.13s(2.42s),835.59Ns(743.94Ns), 1.06MPa(0.76MPa), 1.48MPa(1.43MPa).

The predicted thrust, maximum thrust, specific impulse, the propellant burn time, the total impulse, the average chamber pressure and maximum chamber pressure values for Star grain geometry as presented in Table 7 are 370.71N, 611.67N, 97.97s, 2.22s,812.32Ns,1.00MPa, 1.65MPa. While the empirical values are 313.79N, 581.16N, 88.06s, 2.34s,734.26Ns, 0.78MPa, 1.45MPa. Similarly, the measured performance parameters for Rod and Tube propellant grain geometry are gives as 215.50N, 285.63N,87.87s, 3.4s,732.71Ns,0.56MPa, 0.75MPa as compared to its predicted values: 265.02N, 306.87N,99.43s,3.15s,833.27Ns,0.76MPa, 0.88MPa (Tables 8). The comparative descriptions of both the theoretical predictions and measured parameters relatively among the four selected propellant grain geometries are presented in Table 9 and Table 10 respectively. While the Figure 12 shows their comparative thrust profiles.

Table 5 Bate Grain Geometry Ballistic Performance Parameters

S/N	Grain Parameters	Units	Simulation Values	Validation Values	Percent error (%)
1	Total Impulse	Ns	830.89	747.75	10.01
2	Specific impulse, Isp	s	99.76	89.67	10.11
3	Propellant burn time	s	3.15	2.74	13.02
4	Average thrust	N	261.54	272.90	4.34
5	Maximum thrust	N	303.38	324.35	6.91
6	Average pressure	MPa	0.75	0.72	4.00
7	Maximum pressure	MPa	0.87	0.85	2.30
8	Ideal thrust coefficient	-	1.11	1.2	8.11

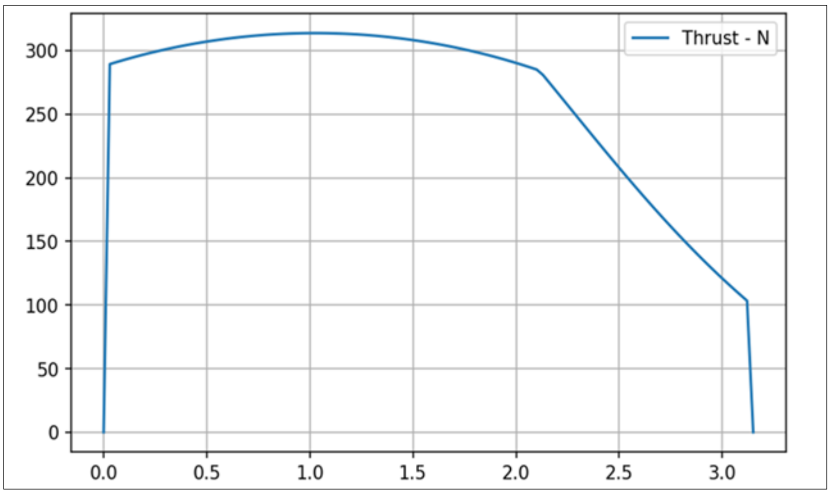

Figure 4 Predicted thrust profiles for Bate grain geometry

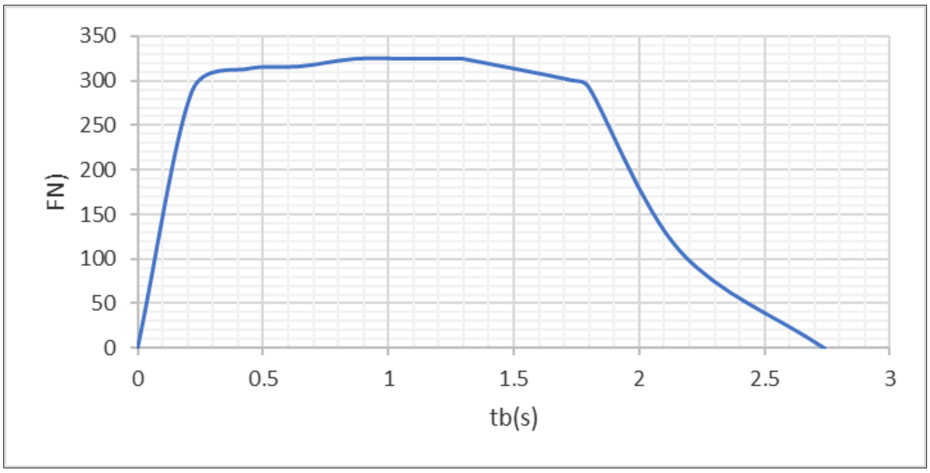

Figure 5 The delivered thrust profiles for Bate grain geometry

Table 6 Finocyl Grain Geometry Ballistic Performance Parameters

S/N	Grain Parameters	Units	Simulation Values	Validation Values	Percent error (%)
1	Total Impulse	Ns	835.59	743.94	10.97
2	Specific impulse, Isp	s	100.36	89.21	11.11
3	Propellant burn time	s	2.13	2.42	13.62
4	Average thrust	N	396.28	307.41	22.43
5	Maximum thrust	N	553.30	573.63	3.67
6	Average pressure	MPa	1.06	0.76	28.30
7	Maximum pressure	MPa	1.48	1.43	3.38
8	Ideal thrust coefficient	-	1.19	1.28	7.56

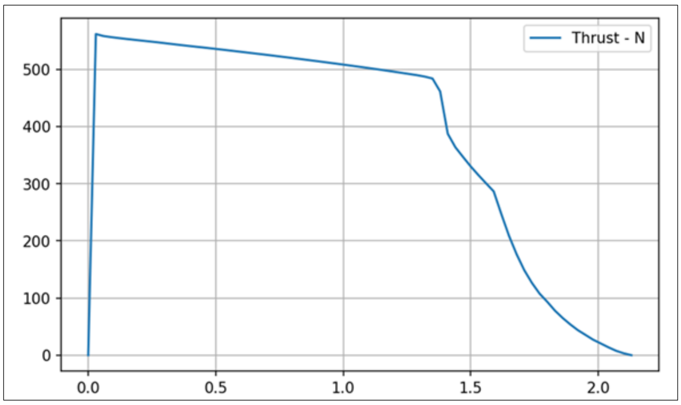

Figure 6 Predicted thrust profiles for Finocyl grain geometry

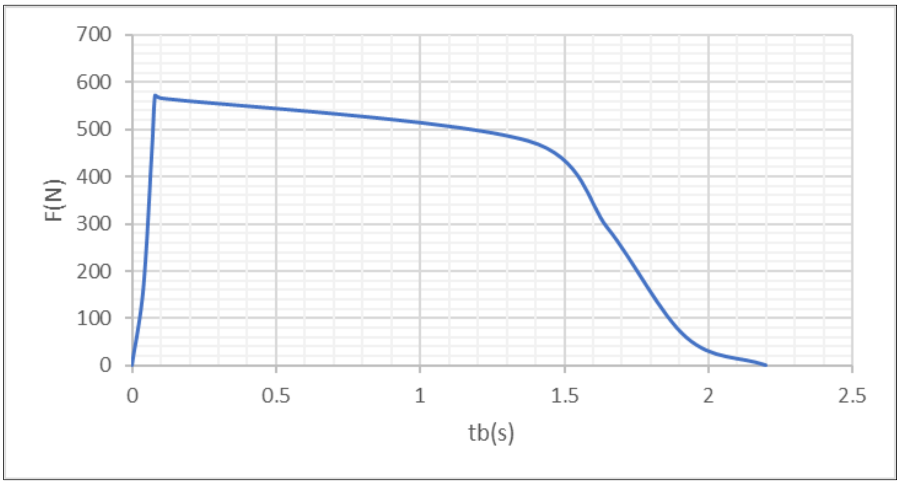

Figure 7 The delivered thrust profiles for Finocyl grain geometry

Table 7 Star Grain Geometry Ballistic Performance Parameters

S/N	Grain Parameters	Units	Simulation Values	Validation Values	Percent error (%)
1	Total Impulse	Ns	812.32	734.26	9.61
2	Specific impulse, Isp	s	97.97	88.06	10.12
3	Propellant burn time	s	2.22	2.34	5.41
4	Average thrust	N	370.71	313.79	15.35
5	Maximum thrust	N	611.67	581.16	4.99
6	Average pressure	MPa	1.00	0.78	22.00
7	Maximum pressure	MPa	1.65	1.45	12.12
8	Ideal thrust coefficient	-	1.18	1.27	7.63

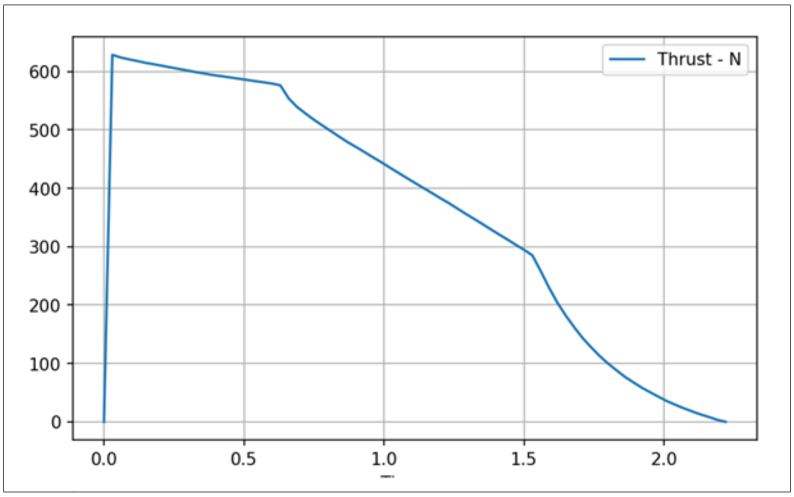

Figure 8 The predicted thrust profiles for Star grain geometry

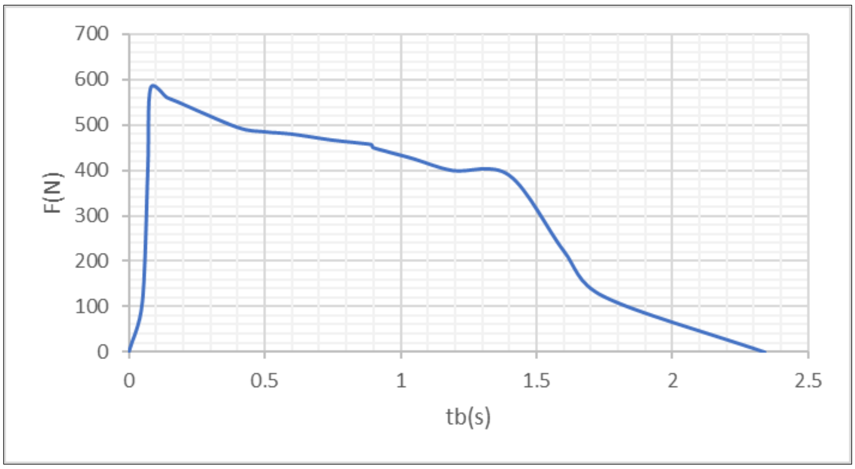

Figure 9 The delivered thrust profiles for Star grain geometry

Table 8 Rod and Tube Grain Geometry Ballistic Performance Parameters

S/N	Grain Parameters	Units	Simulation Values	Validation Values	Percent error (%)
1	Total Impulse	Ns	833.27	732.71	12.07
2	Specific impulse, Isp	s	99.43	87.87	11.63
3	Propellant burn time	s	3.15	3.4	7.94
4	Average thrust	N	265.02	215.50	18.69
5	Maximum thrust	N	306.87	285.63	6.92
6	Average pressure	MPa	0.76	0.56	26.32
7	Maximum pressure	MPa	0.88	0.75	14.77
8	Ideal thrust coefficient	-	1.17	1.2	2.56

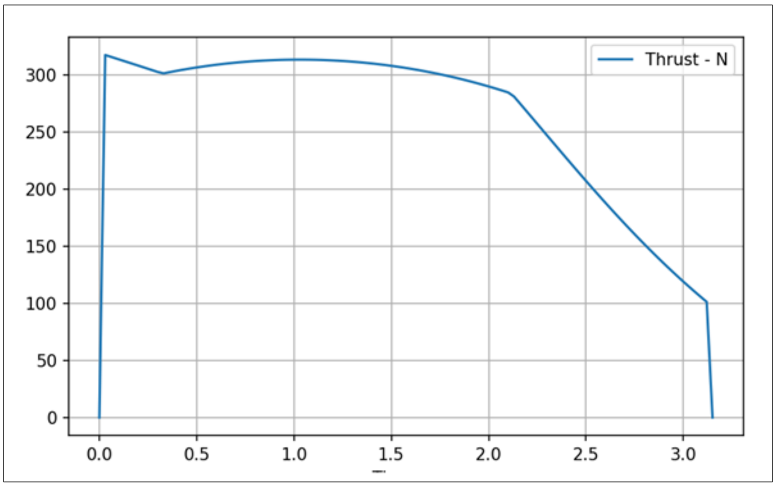

Figure 10 The predicted thrust profiles for Rod and Tube grain geometry

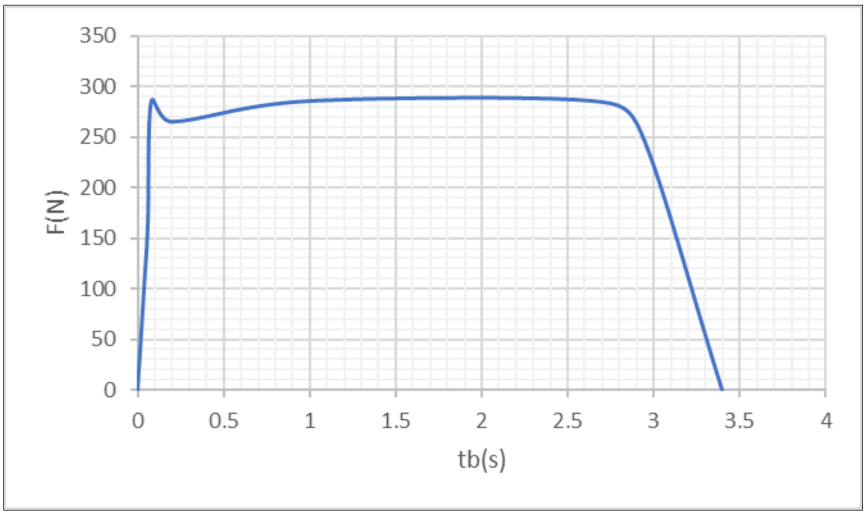

Figure 11 The delivered thrust profiles for Rod and Tube grain geometry

Table 9 The Grain Geometries' Comparative Predicted Ballistic Parameters

S/N	Grain Parameters	Units	BATES	FINOCYL	STAR	ROD & TUBE
1	Total Impulse	Ns	747.75	743.94	734.26	732.71
2	Specific impulse, Isp	s	89.67	89.21	88.06	87.87
3	Propellant burn time	s	2.74	2.42	2.34	3.4
4	Average thrust	N	272.90	307.41	313.79	215.50
5	Maximum thrust	N	324.35	573.63	581.16	285.63
6	Average pressure	MPa	0.72	0.76	0.78	0.56
7	Maximum pressure	MPa	0.85	1.43	1.45	0.75
8	Ideal thrust coefficient	-	1.2	1.28	1.27	1.2
9	Propellant mass	Kg	0.85	0.85	0.85	0.85

Table 10 The Grain Geometries' Comparative Delivered Ballistic Parameters

S/N	Grain Parameters	Units	BATES	FINOCYL	STAR	ROD &TUBE
1	Total Impulse	Ns	830.89	835.59	812.32	833.27
2	Specific impulse, Isp	s	99.76	100.36	97.97	99.43
3	Propellant burn time	s	3.15	2.13	2.22	3.15
4	Average thrust	N	261.54	396.28	370.71	265.02
5	Maximum thrust	N	303.38	553.30	611.67	306.87
6	Average pressure	MPa	0.75	1.06	1.00	0.76
7	Maximum pressure	MPa	0.87	1.48	1.65	0.88
8	Initial Kn	-	55.63	122.44	137.40	62.23
9	Maximum kn	-	61.04	122.44	137.40	62.23

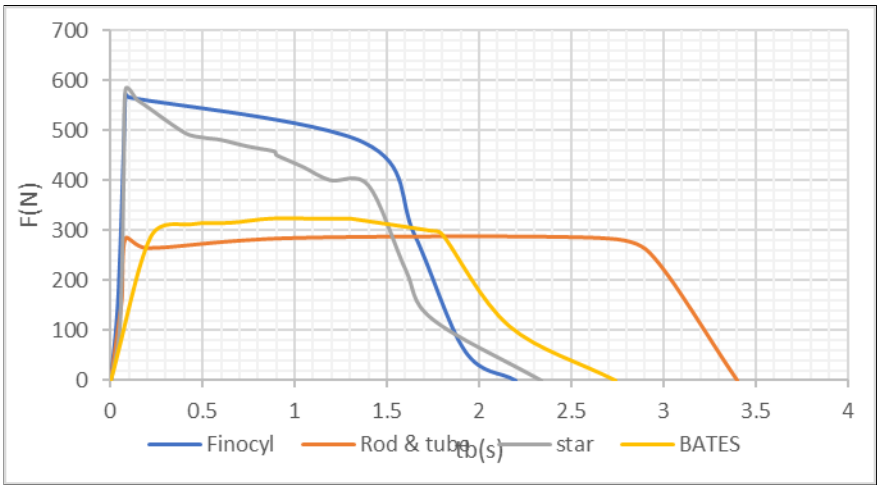

Figure 12 Comparison of experimental validated thrust curves of the four (4) different propellant grain geometries design

The results demonstrate the distinct burn dynamics of various propellant grain geometries and their direct impact on motor and ballistic performance. Grain geometry critically dictates the evolution of the burning surface area during combustion. Because chamber pressure drives the burn rate, and pressure is inherently linked to the available burning area, geometry ultimately governs overall motor performance. Bate grain produced neutral thrust profiles. The burning area stays almost constant as the hole gets bigger. Inner radius increases, but length stays same, so the thrust is approximately constant over burn time. The simultaneous regression of the inner core and outer surfaces resulted in a nearly constant burning area throughout most of the burn. This is suggested for a steady, predictable thrust most used in boosters.

The Finocyl propellant grain geometry exhibits a distinct, mildly progressive to regressively-neutral burn pattern. Initially, the extensive surface area of the fins drives a high burning rate, generating a sharp spike in early thrust. As these fins erode, the geometry transitions toward a standard cylindrical perforation, causing the burning surface area to drop and stabilize. This structural evolution results in a characteristic progressive-regressive-neutral profile-marked by a high initial peak followed by a sustained, flatter thrust curve. Consequently, the Finocyl configuration is ideally suited for tactical missile applications that require rapid off-the-pad acceleration followed by a steady cruise or sustain phase. Upon ignition, combustion occurs simultaneously along the Star points and their corresponding valleys, providing an expansive initial surface area that generates a sharp thrust spike and accelerated energy release. As regression progresses, the Star points erode rapidly, causing a sharp decline in the burning surface area and a corresponding drop in thrust. Once the star geometry is completely consumed, the perforation transitions into a simple cylindrical core. At this stage, the grain mimics the neutral, steady thrust profile of a Bate grain, where the burning area stabilizes for the remainder of the burn. This progressive-short-neutral-regressive behavior is highly effective for air-to-air missiles that require rapid rail separation followed by sustained velocity. The Rod and Tube propellant grain geometry, is associated with burning from small surfaces simultaneously. As each rod burns inward, its surface area decreases. The thrust profile is regressive and thrust starts high, continuously decreases. This is good for motor specific impulse tailoring.

The ballistic performance of the rocket motor closely mirrored the trends established by the variations in burning surface area. The star grain configuration exhibited an abrupt rise in chamber pressure, achieving the highest peak among the four evaluated geometries due to its rapidly expanding initial surface area. Conversely, the Finocyl grain demonstrated a moderate pressure increase followed by a stable burn phase, indicating controlled combustion with a minimized risk of pressure spikes. Both the Bate grain and the Rod-and-Tube grain displayed neutral burning characteristics, maintaining relatively constant chamber pressures with negligible fluctuations. However, while the Rod-and-Tube geometry shared this stable profile, it operated at a lower pressure magnitude than the tube grain because of its smaller effective burning area. The thrust-time curves clearly illustrate the profound influence of propellant grain geometry on the rocket motor's ballistic performance. The Star grain exhibited a progressive, near-neutral burning thrust profile, characterized by a significant post-ignition increase that peaked near mid-burn before declining. Conversely, the Bate grain demonstrated a highly uniform, neutral profile, maintaining nearly constant thrust throughout the combustion duration. The Finocyl grain produced a relatively flat, near-neutral curve with minor progression, balancing high initial thrust with long-term stability. Similarly, the Rod-and-Tube geometry delivered a stable, neutral thrust profile with minimal variation, though it operated at a lower overall magnitude than the tube grain due to its smaller effective burning area. Ultimately, the thrust analysis confirms that the Star grain generates the highest maximum thrust, the Finocyl grain optimizes thrust uniformity with moderate enhancement, and both the Bate and Rod-and-Tube configurations ensure stable, steady-state thrust.

A comparative evaluation of ballistic performance was conducted across the geometries. In terms of thrust magnitude and burn duration, the Star grain delivered the highest peak thrust but exhibited the shortest burn time due to rapid propellant consumption. Conversely, the Bate grain produced a highly consistent thrust profile and excellent burn efficiency, cementing its status as one of the most widely utilized geometries in solid rocket motors. The Finocyl grain provided a balanced performance characterized by a moderate peak thrust and a sustained burn duration. Finally, the Rod-and-Tube grain achieved the longest overall burn duration with stable thrust, albeit at a lower delivered ballistic magnitude compared to the other configurations. The results confirm that grain geometry is a dominant factor in internal ballistics evaluation. The observed performance variations stem directly from how each configuration governs the rate of change of the propellant's burning surface area. An expanding surface area increases the mass flow rate, thereby elevating chamber pressure and delivered thrust, whereas a constant surface area yields a stable mass flow rate, producing steady pressure and thrust. Mechanistically, the sharp edges of the Star grain accelerate exposed surface area growth, whereas the fins of the Finocyl grain regulate surface evolution. Meanwhile, the Bate and Rod-and-Tube geometries maintain a precise balance between internal and external burning surfaces, ensuring stable, neutral performance.

4. Conclusion

The research established how solid rocket motor performance is directly engineered through rocket propellant grain geometry. By controlling how the burning surface area evolves during combustion, the geometry fundamentally dictates mass flow rate, chamber pressure, and thrust stability. It also established that Star grain geometry is suitable for maximum peak thrust and rapid initial energy release. For an optimized balance of rapid off-the-pad acceleration and sustained cruise, the Finocyl grain offered the best progressive-near neutral profile. For solid rocket motor thrust stability and predictability, the Bate and Rod-and-Tube grains remain unmatched, with the latter trading peak performance for maximum burn longevity. These distinct ballistic behaviours confirm that grain geometry selection is the most critical variable in matching solid rocket motor capabilities to specific tactical and booster mission requirements. A proper understanding and application of geometric effects enable engineers to tailor motor performance to specific mission needs, ensuring efficiency, safety, and reliability.

Compliance with ethical standards

Acknowledgments

We acknowledged the efforts and contributions of the members of staff of the Rocket Propellant Development Systems Division, the Bola Ahmed Tinubu Centre for Space Transport and Propulsion (BATCSTP), Epe, Lagos, Nigeria, for their assistance throughout the investigation.

Disclosure of conflict of interest

There are no conflicts of interest.

References

[1] Sutton, G. P., and Biblarz, O. (2017). Rocket propulsion elements (9th ed.). Wiley.

[2] Humble, R. W., Henry, G. N., & Larson, W. J. (1995). Space propulsion analysis and design. McGraw-Hill.

[3] Gupta, A., Nair, P., Ashish, A. S., and Abraham, B. C. (2020). Numerical study of impact of grain profile on the internal ballistics of solid rocket motor. Journal of Aerospace Engineering and Technology.

[4] Nehal, A., & Venkatachalam, N. V. (2024). Grain design and geometrical analysis and burn rate of rocket motors. International Journal of Progressive Research in Engineering Management and Science.

[5] Chiaverini, M. J., and Kuo, K. K. (Eds.). (2007). Fundamentals of hybrid rocket combustion and propulsion. American Institute of Aeronautics and Astronautics.

[6] Greatrix, D. R. (2012). Powered flight: The engineering of aerospace propulsion. Springer.

[7] Karakas, H., and Ak, M. A. (2021). Parametric analysis of solid rocket motor performance for different grain geometries using analytical burn-back methods. Aerospace, 8(9), 255.

[8] Li, W., Li, W., He, Y., and Liang, G. (2022). Reverse design of solid propellant grain for a performance-matching goal.

[9] Mukunda, H. S. (2012). Understanding aerospace chemical propulsion. Interline Publishing.

[10] Nehal, A., and Venkatachalam, N. V. (2024). Grain design and geometrical analysis and burn rate of rocket motors. International Journal of Progressive Research in Engineering Management and Science, 4(11), 1593–1605. Okninski, A., Kopacz, W., Kaniewski, D., & Sobczak, K. (2021). Solid rocket propulsion technology for de-orbiting spacecraft — review of the state of the art with applications.

[11] Petrarolo, A., Kobald, M., and Schlechtriem, S. (2018). Understanding the combustion process in hybrid rocket propulsion. Acta Astronautica, 158, 313–322.

[12] Scippa, S., Pascal, P., and Zanier, F. (2014). Pressure oscillations and structural response in solid rocket motors: An experimental and numerical study. Progress in Aerospace Sciences.

[13] Sutton, G. P., and Biblarz, O. (2017). Rocket propulsion elements (9th ed.). Wiley.

[14] Tola, C. (2018). Zero-dimensional internal ballistic solver for solid rocket motor design validation. Journal of Propulsion and Power.

[15] eorgia Korompili, Günter Mußbach, and Christos Riziotis (2024). Structural Health Monitoring of Solid Rocket Motors: From Destructive Testing to Perspectives of Photonic Based Sensing. Instruments 2024, 8(1),16; https://doi.org/10.3390/instruments8010016.

[16] Magdi Abelrazig Elhag Mohamed, Mohamed Eltayeb Mansour (2018). Simulation of Internal Ballistics Solid Rocket Motor. European Academic Research Vol. V, Issue 12, 2286-4822.

[17] Ashraf Nehal and N. Venkatachalam (2024). Grain Design and Geometrical Analysis and Burn Rate of Rocket Motors. International Journal of Progressive Research in Engineering Management and Science (Int Peer Reviewed Journal), Issue: 11, Volume: 04, 1593-1605. https://doi.org/10.58257/IJPREMS36994.